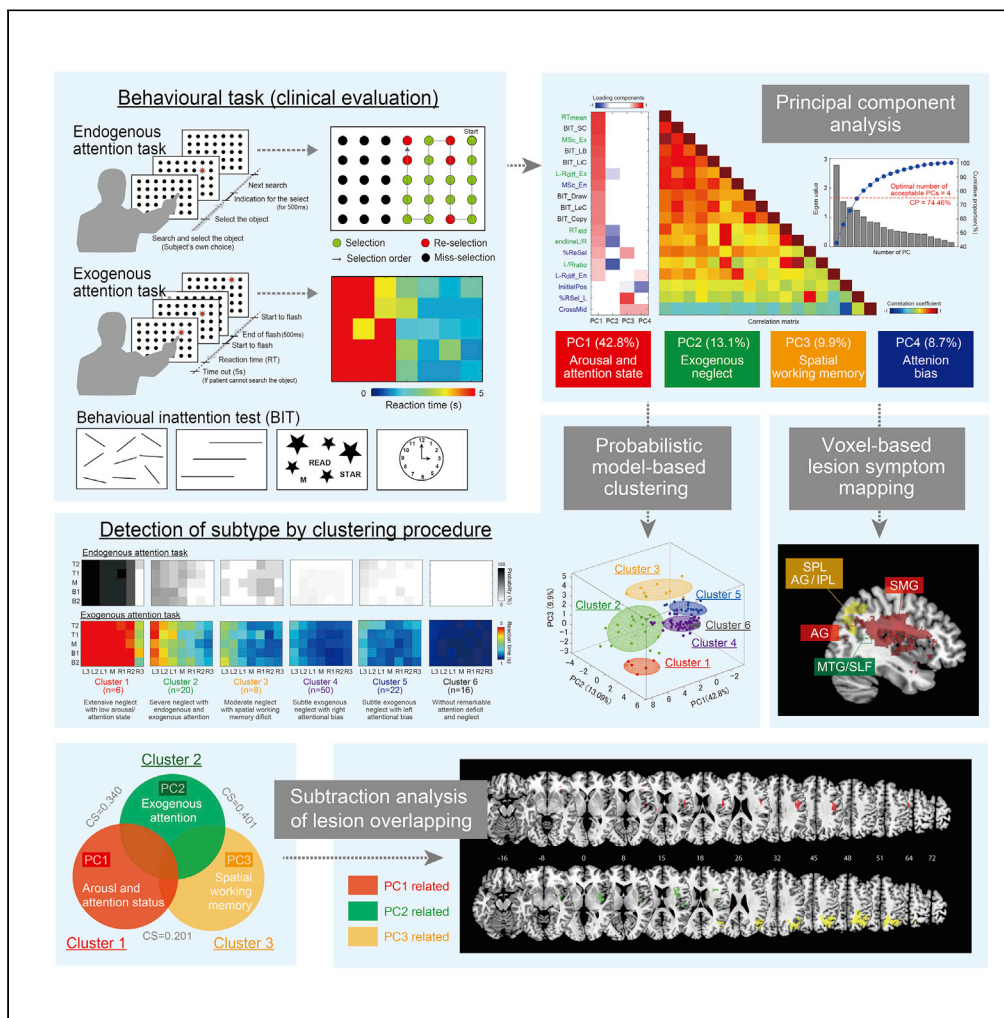**Article**

Pathological structure of visuospatial neglect: A comprehensive multivariate analysis of spatial and non-spatial aspects

Yusaku Takamura,
Shintaro Fujii,
Satoko Ohmatsu,
Shu Morioka,
Noritaka Kawashima

nori@rehab.go.jp

Highlights

This study attempted to establish the pathological structure of visuospatial neglect

PCA revealed four distinct fundamental components underlying visuospatial neglect

GMM-based clustering detected six subtypes of visuospatial attention network deficit

iScience

Article

Pathological structure of visuospatial neglect: A comprehensive multivariate analysis of spatial and non-spatial aspects

Yusaku Takamura,[1,2] Shintaro Fujii,[2,3] Satoko Ohmatsu,[1] Shu Morioka,[2,4] and Noritaka Kawashima[1,*]

SUMMARY

Visuospatial neglect (VSN) is a neurological syndrome of higher brain functions in which an individual fails to detect stimuli on a space that is contralateral to a hemispheric lesion. We performed a comprehensive multivariate analysis based on the principal component analysis (PCA) and cluster analysis in patients with right hemisphere stroke and then performed a determination of different elements of VSN. PCA-based cluster analysis detected distinct aspects of VSN as follows: cluster 1: low arousal and attention state, cluster 2: exogenous neglect, cluster 3: spatial working memory (SWM) deficit. Lesion analysis revealed neural correlates for each cluster and highlighted "disturbance of the ventral attention network" for the stagnation of exogenous attention and "parietal damage" for SWM deficit. Our results reveal a pathological structure of VSN as multiple components of an attention network deficit, and they contribute to the understanding of the mechanisms underlying VSN.

INTRODUCTION

Visuospatial processing is a fundamental aspect of human cognitive behavior. Neurophysiological studies have attempted to reveal the nature of the neural mechanisms underlying visuospatial attention and have yielded insights into the global structure of neural networks involved in multi-modal and a wide range of components of neural processing. In 2002, Corbetta and Shulman (Corbetta and Shulman 2002) identified two distinct forms of attentional pathway: one is a dorsal pathway, with connections between the superior parietal lobule (SPL)/the intraparietal sulcus and the frontal eye field, and the other is a ventral pathway, with connections between the temporo-parietal junction and the middle frontal gyri (MFG) and inferior frontal gyri (IFG). The dorsal pathway is known as the dorsal attention network (DAN), which is associated mainly with goal-directed selection (Corbetta and Shulman., 2002; Gitelman et al., 1999; Kim and Cave, 1999; Rosen et al., 1999; Hopfinger et al., 2000; Beauchamp et al., 2001). The ventral pathway is known as the ventral attention network (VAN), and it is suspected to mediate shifts of attention when triggered by unattended or unexpected stimuli. From the functional point of view, the DAN is a high-level form of "top-down" endogenous attention to locations or features, and the VAN is a low-level form of "bottom-up" attention which is elicited by exogenous factors. A persuasive methodology to clarify the mechanisms that underlie the visuospatial attention network is the investigation of causal relationships between neurological symptoms and specific brain lesions. For example, the pathological feature of spatial neglect due to right hemisphere damage could indicate a causal relationship between damaged brain areas and neurological symptoms, as described by Pizzamiglio and his colleagues (Bisiach et al., 1996; Guariglia et al., 1993; Robertson et al., 1997). Studies of patients with visuospatial neglect (VSN) have also shed light on the network of brain areas that may be involved in normal spatial cognition and attention, based on the lesions that are typical in neglect. Neglect symptom was classically regarded as a parietal syndrome, but it has become evident as a widespread attention network disorder (Corbetta and Shulman., 2011; Doricchi et al., 2008; Verdon et al., 2010; Karnath and Rorden, 2012; Bartolomeo et al., 2012). While distinct components of VSN have been identified, such as sustained attention deficit (Robertson et al., 1997; Karnath 1988; Rengachary et al., 2011), spatial working memory (SWM) deficit (Malhotra et al., 2009; Husain et al., 2001; Toba et al., 2018), magnetic attraction (Toba et al., 2018; Saj et al., 2018), and perceptive/visuo-spatial, exploratory/visuo-motor, and allocentric/object-centered aspects of neglect (Verdon et al., 2010), VSN can be regarded as a multi-component and the wide range attention network disorder. It is evident that a wide range of symptomatic heterogeneity in patients with VSN can be largely attributed to

[1]Department of Rehabilitation for the Movement Functions, Research Institute of National Rehabilitation Center for Persons with Disabilities, 4-1 Namiki, Tokorozawa, Saitama, Japan

[2]Graduate School of Health Science, Kio University, Nara, Japan

[3]Nishiyamato Rehabilitation Hospital, Nara, Japan

[4]Neurorehabilitation Research Center, Kio University, Nara, Japan

*Correspondence: nori@rehab.go.jp

https://doi.org/10.1016/j.isci.2021.102316

multi-component deficits including the widespread visuospatial attention network. Husain (2019) recently described that none on their own is likely to lead to the full-blown syndrome. Different individuals might have different combinations of deficits depending upon the extent of their brain lesion.

In the present study, we evaluated three elements of VSN in 122 patients who had suffered a right hemisphere stroke: sustained attention, exogenous/endogenous attention, and SWM. Based on a variety of evaluation parameters, we first performed a principal component analysis (PCA) of selected variables obtained across three tests. PCA has been recently utilized to reveal individual's neurological behavior into main component (Corbetta et al., 2015). This analysis process was designed to break down neglect symptom into coherent profiles of co-varying deficits; the PCA results provided four extracted principal components (PCs) that explain 74.46% of the total variance. We then performed a Gaussian mixture model (GMM)-based clustering using four PC scores to discover the distinct type of VSN. As the result, we categorized six distinct clusters by conducting a multivariate analysis. Each cluster can be regarded as a "subtype" of VSN which consists of different contribution of the four PCs.

In order to confirm the above mentioned behavioral characterization, the brain areas responsible for symptomatic features were detected by using a subtraction analysis of brain lesions overlapping among the clusters and voxel-based lesion symptom mapping (VLSM) by the four detected PCs. The analyses revealed specific neural correlates for each of the symptomatic components, and they highlighted "disturbance of the VAN" for the stagnation of exogenous attention and "parietal area damage" for SWM deficit. Another important finding was that the patients' neurological symptoms and functional deficits after they suffered lesions were affected not only by disturbance of the attention network (which was lesion specific) but also by compensation for the symptoms/deficits over time. Our classification includes not only lesion-specific symptoms but also elements concerning compensation (i.e., intentional bias to neglected space). We provide the longitudinal data of four representative patients as part of a discussion of how symptoms change with the time course of recovery.

To the best of our knowledge, this is the first study to establish a pathological structure of VSN using comprehensive multivariate analyses based on various aspects of a clinical evaluation. Our results indicate that the clinical manifestations of VSN might reflect a combination of distinct components affecting different aspects of spatial and non-spatial symptoms.

RESULTS

A total of 122 patients were enrolled in this cross-sectional retrospective study. Figure 1A shows the analytical procedures used in this study. All the patients performed a touch-panel choice reaction task on a personal computer's monitor, and they completed the Behavioral Inattention Test (BIT; Wilson et al., 1987). The touch-panel choice reaction task consisted of an endogenous attention task (EndoAT) and an exogenous attention task (ExoAT). The EndoAT was used for the evaluation of the patients' endogenous attention, SWM, and selection strategy (see Figure 1A and Table 1). With the patient's results on the three evaluation tasks (i.e., the EndoAT, ExoAT, and BIT), we quantified each of the six variables for the subsequent analysis. We then subjected the data to the following three adjustments for the subsequent exploratory/data-driven analysis: (a) dimensional reduction from 18 variables using PCA to elucidate the neglect-related deficit components; (b) GMM-based probabilistic clustering using the four obtained PCs to elucidate different combinations of neglect-related components for each patient; and (c) lesion overlap subtraction of each cluster and VLSM for the four obtained PCs in order to understand the neural mechanisms underlying the neglect-related symptomatic components.
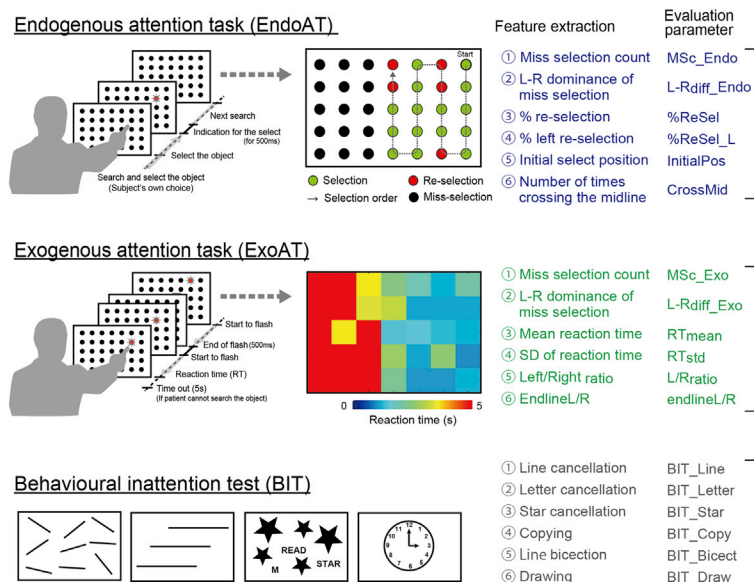
Principal component analysis

The top panel of Figure 1C shows the eigen value (loadings) of each PCs and cumulative proportion obtained by the PCA for the dimensional reduction from the 18 quantified variables. The optimal number of acceptable PCs based on two criteria is four PCs (see the methods). The middle panel of Figure 1C shows a result of the analysis of the loadings of the four acceptable PCs and the correlation matrix between all variables. The results show that the PCs each have a characteristic loading based on the correlation structure between the variables.

The PCs could be reasonably interpreted based on the previous findings as follows. PC1 was interpreted as arousal and attention state, including sustained attention, exploratory neglect, and severity of neglect. This

A Data analysis procedure
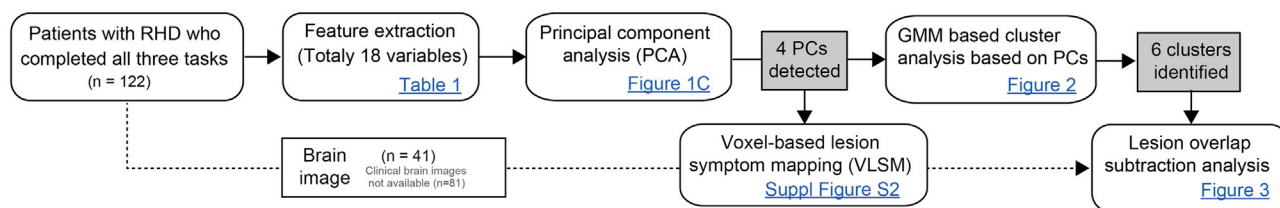
B Multimodal evaluation and parameters

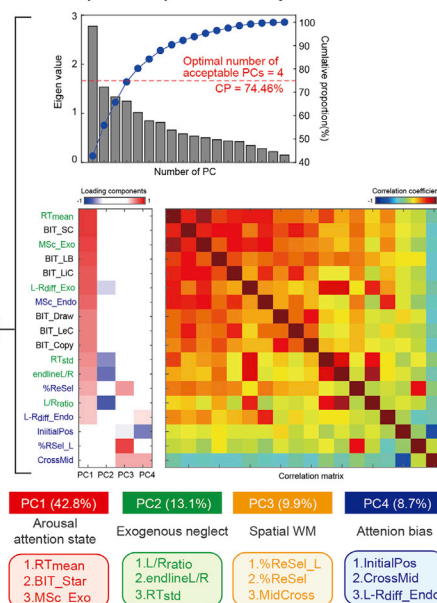**C** Principal component analysis

Figure 1. Framework of this study

(A) Flow chart of data analysis procedure in this study.

(B) Evaluation task and variables for visuospatial neglect. All patients performed touch-panel personal computer (PC)-based choice reaction task and completed the Behavioral Inattention Test (BIT). The endogenous attention task (EndoAT) on the PC was administered to evaluate the patient's endogenous attention spatial working memory (SWM) and selection strategy. The patient was asked to choose all targets in any order. The exogenous attention task (ExoAT) was administered to evaluate the patient's exogenous attention and sustained attention. The patients were instructed to choose a randomly flashed target, and we then calculated the evaluated parameters based on the spatial distribution of the patients' reaction times. The BIT consisted of a line cancellation test, letter cancellation test, star cancellation test, copying test, drawing test, and line bisection test. Using the results of these three evaluation tasks, we quantified six variables in a subsequent analysis.

(C) Principal component analysis (PCA). Top: Eigen value (loadings) of each principal components (PCs) (bar) and cumulative proportion (line) calculated by the PCA for dimensional reduction from 18 quantified variables. Middle: Results of loading values to the four extracted PCs and the correlation matrix between all variables. Each PC could be reasonably interpreted based on previous studies' findings as follows. PC1 was interpreted as arousal and attention state including sustained attention, exploratory neglect, and severity of neglect. PC2: neglect with exogenous attention. PC3: SWM and selection order. PC4: attention bias and selection order.

component had large contributions from mean reaction time in ExoAT (RTmean), star cancellation test in BIT (BIT_SC), and mis-selection count in ExoAT (MSc_Ex). PC2 was interpreted as neglect with exogenous attention. This component had large contributions from the ratio of the reaction time in the left hemispace to that in the right hemispace in ExoAT (L/Rratio) and the standard deviation of the reaction time in ExoAT (RTstd). PC3 was interpreted as SWM deficit and selection order. This component had large contributions from mainly overall space and the left space reselection rate of EndoAT (%ReSel and &ReSel left) and the number of midline crossings in EndoAT (CrossMid). PC4 was interpreted as attention bias and selection order. This component had large contributions from mainly the initial selection position in EndoAT (Initial-Pos), MidCross, and difference of mis-selection count between the left and right hemispace in EndoAT (L-Rdiff_En). We used the PC scores for the detection of subtypes, symptom-specific brain areas with VLSM, and subtraction analysis via cluster analysis.

Table 1. Characteristics of each variable

	Variable	Task	Calculation	Range	Meaning
1	MSc_En	EndoAT	Total targets—count of total selection	0–35	Total capacity for endogenous attention.
2	L-Rdiff_En	EndoAT	MSc_En in left hemispace – MSc_En in right hemispace	−15–15	Neglect in endogenous attention: L-Rdiff_En = 0 indicates no difference between the left and right spaces.
3	%ReSel	EndoAT	Count of reselection/count of total selection * 100	0–100	Spatial working memory: %ReSel = 100% indicates the reselection of all targets.
4	%ReSel_L	EndoAT	Count of reselection in left space/count of total selection in left space * 100	0–100	Spatial working memory in left space: %ReSel_L = 100 indicates reselection of all left targets.
5	InitialPos	EndoAT	Initially selected position (the left top target is 1 and the right bottom target is 35.)	1–35	Exploration strategy.
6	CrossMid	EndoAT	No. of midline crossings (excluding RS target)	Inf	Exploration strategy.
7	MSc_Ex	ExoAT	No. of targets—count of total selection	0–35	Total ability of exogenous attention.
8	L-Rdiff_Ex	ExoAT	MSc_Ex in left hemispace – MSc_Ex in right hemispace	−15–15	Neglect in exogenous attention: L-Rdiff_Ex = 0 indicates no difference between left and right space.
9	RTmean	ExoAT	Mean reaction time	Inf	Sustained attention.
10	RTstd	ExoAT	Standard deviation of reaction time	Inf	Variability of attention, sustained attention
11	L/Rratio	ExoAT	Mean reaction time in the left hemispace/ Mean reaction time in the right hemispace	Inf	Neglect in exogenous attention: L/Rratio = 1 indicates no difference between left and right space.
12	EndlineL/R	ExoAT	Mean reaction time in the left end column/ Mean reaction time in the right end column	Inf	Neglect in exogenous attention: EndlineL/R = 1 indicates no difference between left and right end line.
13	BIT_Line	BIT	Count of total cancellation (conventional evaluation method)	0–36	Score of the line cancellation test in BIT: Explorational neglect.
14	BIT_Letter	BIT	Count of total cancellation (conventional evaluation method)	0–40	Score of the letter cancellation test in BIT: Explorational neglect.
15	BIT_Star	BIT	Count of total cancellation (conventional evaluation method)	0–54	Score of the star cancellation test in BIT: Explorational neglect.
16	BIT_Copy	BIT	No. of complete (conventional evaluation method)	0–4	Score of the copying test in BIT: Visual neglect and construction.
17	BIT_Bicect	BIT	Deviation is divided into three score areas (conventional evaluation method)	0–9	Score of the line bisection test in BIT: Degree of deviation in neglect space.
18	BIT_Draw	BIT	No. of complete (conventional evaluation method)	0–3	Score of the drawing test in BIT: Visual neglect and construction.

Gaussian mixture model-based cluster analysis

To classify the subtypes of VSN, we used the PC scores for a GMM-based clustering. We selected the model showing high theoretical validity with a better Bayesian information criterion (BIC) and integrated complete-data likelihood (ICL) as the optimal model from among several models that met these criteria (see Table S1 for details). We detected six clusters from the 60 candidate models. The percentages of each cluster's members are shown as a pie chart in Figure 2A. The averaged PC scores in each cluster are presented as a color matrix in Figure 2A. Details of the basic attributes in each cluster are listed in Table 2.

Figure 2B is scatter plots of PC1 to PC3 in each cluster with 10%–90% confidence ellipsoids and ellipses. The three-dimensional plot and 90% confidence ellipsoids of PC1 to PC3 illustrate the independence and characteristics of each cluster. The PC1 and PC2 planes showed inverse U-shaped distributions, and each cluster is placed along clusters of high to low severity. In contrast, clusters 2 and 3 on the PC1 and PC3 planes are split in the domain of PC3. A statistical comparison of the scores among clusters was performed separately for each of the main three PCs in Figure 2C. The score of PC1 was significantly larger in cluster 1 than in the other clusters and significantly larger in clusters 2 and 3 than in clusters 4–6 and significantly larger in cluster 4 than in clusters 5 and 6 ($\chi2 = 84.726$, df = 5, p = 8.59×10^{-17}, r = 0.728). The score of PC2 was significantly smaller in cluster 2 compared to clusters 1, 4, 5, and 6 without cluster 3. Cluster 1 was significantly larger than the other clusters ($\chi2 = 43.505$, df = 5, p = 2.919×10^{-8}, r = 0.502). PC3 was significantly
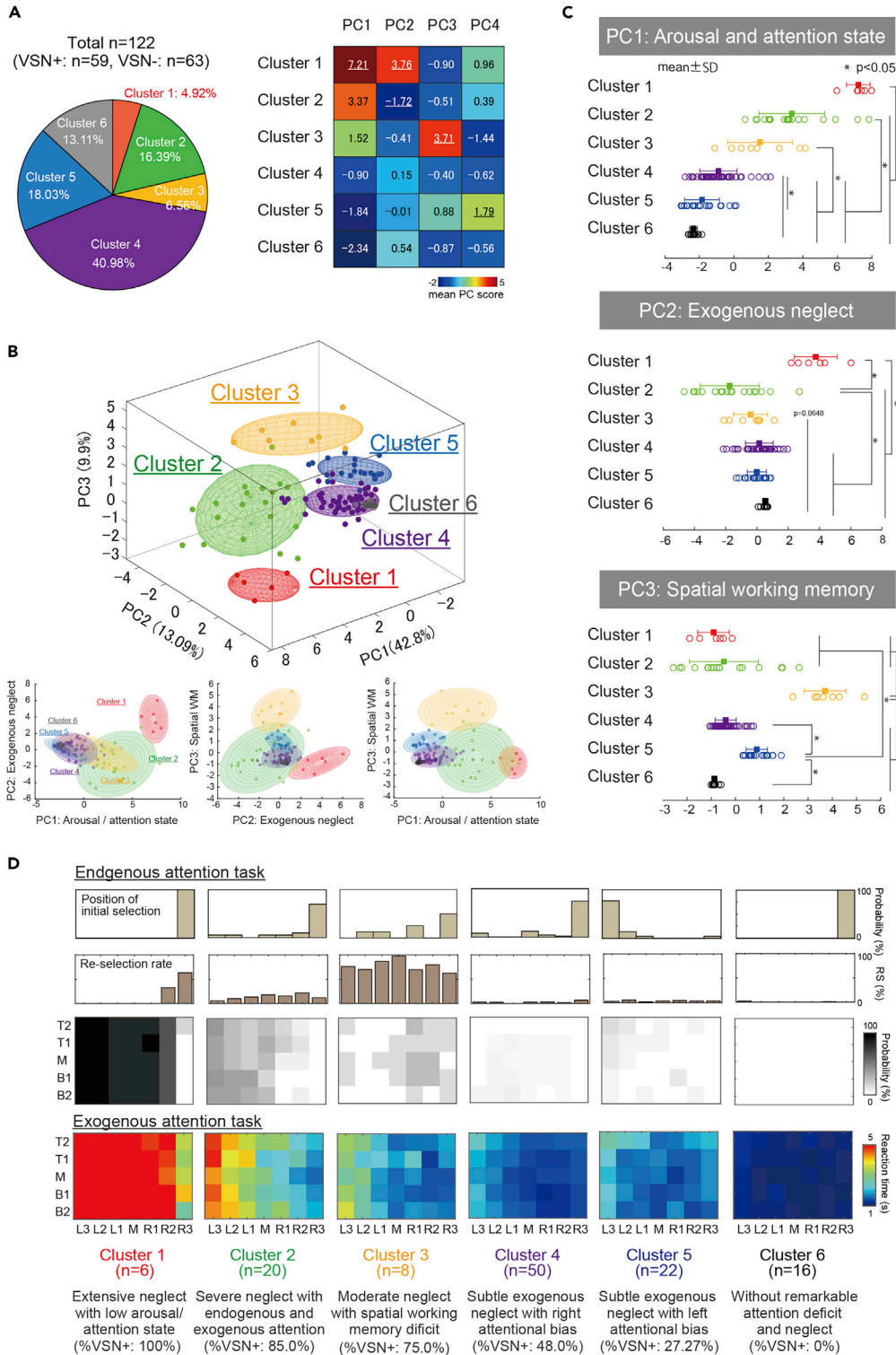
Figure 2. Summary of the Gaussian mixture model (GMM)-based cluster analysis

(A) The percentages of each cluster's members are shown as a pie chart. Six patients (4.92%) were classified as cluster 1, 20 patients (16.39%) as cluster 2, eight (6.56%) as cluster 3, 50 (40.98%) as cluster 4, 22 (18.03%) as cluster 5, and 16 (13.11%) as cluster 6. The averaged PC scores in each cluster are presented as a color matrix.

Figure 2. Continued

(B) Scatterplots of PC1 to PC3 in each cluster with 10%–90% confidence ellipsoids and ellipses. The three-dimensional plot and 90% confidence ellipsoids of PC1 to PC3 show the independence and characteristics of each cluster.

(C) Results of the statistical comparison of the scores among clusters, shown separately for each of the main three PCs (top: PC1, middle: PC2, bottom: PC3) from Figure 1C. Data are represented as mean ± standard deviation (SD). Asterisks are represented as statistical significance (p < 0.05) to obtain by post hoc test (Steel-Dwass test) in Kruskal-Wallis test.

(D) Summary of the EnAT and ExAT scores in each cluster. Top row: The proportion of the initial selection position in each cluster at the EnAT. Second row: The re-selection probability in each column. Third row: The spatial distribution of selection probability values in the EnAT. Fourth row: The spatial distribution of reaction times in the ExAT (red = slow reaction time).

larger in cluster 2 than in the other clusters and significantly larger in cluster 5 than in the other clusters ($\chi 2 =$ 69.113, df = 5, p = 1.568 × 10^{-13}, r = 0.668). The detailed statistical results are provided in Table S2.

Figure 2D illustrates the summarized EndoAT and ExoAT results in each cluster, including the proportion of the initial selection position in each cluster at the EndoAT and the re-selection probability. The spatial distributions of selection probability in the EndoAT and the reaction times in ExoAT are illustrated. Each cluster shows different results for each evaluation point. Cluster 1 can be characterized by extensive neglect with a low arousal/attention state: namely, difficulty of selection in the EndoAT, delayed reaction time not only in the left space but also in the right space, and a high probability of re-selection only in the right space. Cluster 2 can be characterized by severe neglect with endogenous and exogenous attention, i.e., difficulty of selection in the left space in the EndoAT, and extensive delayed response in the left space at the ExoAT.

Cluster 3 can be characterized by moderate neglect with a deficit of SWM; a high probability of re-selections on both the left and right spaces and a moderate extent of delayed response in the left space at the ExoAT. Cluster 4 can be characterized by subtle exogenous neglect with right attentional bias, i.e., a subtle delayed response in the left space at the ExoAT with right attentional bias. Cluster 5 can be characterized by subtle exogenous neglect with left attentional bias: a subtle delayed response in the left space at ExoAT with left attentional bias. Cluster 6 can be characterized as without remarkable attention deficit and neglect, that is, better performance than other clusters in both tasks.

Lesion subtraction analysis for two distinctive clusters

Figure 3A shows the lesion overlapping among 41 of 122 patients. Overlap images of the clusters in which there were brain images of >50% of all cases in the respective cluster are provided in Figure 3A. The three clusters which were applicable had different features in the lesion area.

The Venn diagram in Figure 3A is a schematic representation of the similarities/differences among three PCs based on the pairwise cosine similarity (CS) distance among clusters. The difference of each cluster clearly reflects distinct aspects of VSN as follows: [low arousal and attention state = cluster 1\(cluster 2 ∪ cluster 3), exogenous neglect = cluster 2\cluster 3, SWM = cluster 3\cluster 2]. We used this characterization for the subtraction analysis of the brain lesion overlapping, and we then obtained specific neural correlates for each of these components. The lesions detected by subtracting cluster 1 from clusters 2 plus 3 are shown in Figure 3B. In consideration of the small number of subjects in each cluster and the difficulty of the statistical analysis, we set a criterion of at least 50% difference in overlapped area to minimize overestimation of the detected lesions (Lunven et al., 2015). The dominant lesions in cluster 1 were the insula (68%), the opercular part of the IFG (IFGop; 62%), the orbital part of the IFG (IFGorb; 61%), the superior longitudinal fasciculus (SLF: 57%), and the supramarginal gyrus (SMG: 57%). Figure 3B also shows the lesion detected by subtraction between cluster 2 and cluster 3. The dominant lesion areas in cluster 2 were mainly the insula (50%), the opercular part of IFG (IFGop; 50%), the superior temporal gyrus (STG: 50%), the opercular part of the Rolandic area (Rolandic op; 50%), and the SLF (51%). In contrast, the dominant detected lesions in cluster 3 were mainly the precuneus (PrCUN; 60%), the SLF (66%), the superiror occipital gyrus (SOG: 80%), the angular gyrus (AG: 80%), and the superior and inferior parietal lobules (SPL; 80%, IPL; 73%). The detailed results of the subtraction analysis are summarized in Table S3.

Attention bias (domain of PC4)

PC4 was interpreted as a component of attentional bias and selection strategy (Figure 1D). Figure 4A illustrates the summarized EndoAT and ExoAT results in cluster 4 and 5. Figure 4B showed the comparison of

Table 2. Difference in basic attribution between each cluster

Cluster	n	Age	Sex (F/M)	Time	MMSE	BIT	% VSN	CBS n	Objective	Subjective	Diff
Cluster 1	6	79.5 (54–87)	1/5	33 (3–114)	16.5 (12–27)	26 (16–70)	100%	3	10 (6–15)	1 (1–3)	9 (5–12)
Cluster 2	20	69 (50–80)	7/13	57 (1–673)	22 (16–28)	103 (36–144)	85%	5	11 (10–15)	4 (0–7)	9 (3–11)
Cluster 3	8	68.5 (42–83)	2/6	47.5 (3–240)	23.5 (15–29)	123.5 (64–139)	75%	4	8 (5–9)	3 (1–4)	4 (4–7)
Cluster 4	50	65.5 (34–86)	18/32	46 (2–806)	25 (8–30)	131.5 (32–146)	48%	23	3 (0–15)	1 (0–12)	1 (−2–9)
Cluster 5	22	67 (33–90)	8/14	43.5 (4–265)	28 (13–30)	135.5 (115–146)	27.27%	9	0 (0–10)	0 (0–6)	0 (0–6)
Cluster 6	16	65 (42–86)	5/11	50.5 (4–1653)	29 (24–30)	144 (135–146)	0%	5	0 (0–1)	0	0 (0–1)
All	122	68 (33–90)	41/81	49 (1–1653)	25 (8–30)	131.5 (16–146)	48.36%	49	3 (0–15)	1 (0–12)	1 (-2–12)

The median (min-max) value is shown as a representative value for all variables. MMSE, mini mental state examination; BIT, Behavioral Inattention Test; % VSN, percentage of visuospatial neglect; CBS, Cathrine Bergego Scale; CBSd, difference of CBS.

PC scores among clusters revealed that the score of PC4 was significantly larger in cluster 5 than in the other clusters ($\chi 2 = 65.778$, df = 5, p = 7.729×10^{-13}, r = 0.649). The averaged PC scores in each cluster revealed that the difference between clusters 4 and 5 was particularly clear in PC4, whereas there was little difference in PC1, 2, and 3 (Figure 4C).

Longitudinal analysis of four representative patients

To test our interpretation of each PC and cluster, we observed the recovery process in four representative patients (Figure 5). At the first assessment, case 1 had much difficulty in both task (Figure 5A) and then gradually improved but was still stagnant EndoAT 130 days after stroke. Case 2 also had much difficulty at the first assessment but gradually improved his performance in both tasks, and he could select/respond all targets at 133 days. Patients 3 and 4 commonly showed difficulty of response only in the left space in the ExoAT, but their search behavior in the EndoAT showed a clear difference, i.e., patient 3 searched for the objects in a random order, and patient 4 showed many re-cancellations. Both patients tended to show good recovery within 1-month after stroke. The extent and characteristics of neglect behavior were also clearly reflected in the BIT results (Figure 5A). The time course changes in the patients' BIT total scores are summarized in Figure 5A.

The transition patterns among PCs in each case (Figure 5B) were obtained as a quantitative representation of the characteristic recovery process in the representative cases (each patient showed a different traveling path). The contrast between case 1 and 2 indicates that both cases originated in cluster 1 and then the patient moved to cluster 2 (stagnation of exogenous attention), whereas case 2 moved to cluster 3 (SWM deficit). The contrast between patients 3 and 4 reflects different aspects of the recovery process: both patients finally move to cluster 4, but case 3 originated in cluster 2 (exogenous neglect) and patient 4 originated in cluster 3 (SWM deficit). These representative cases clearly demonstrated a distinct modality of symptoms and different recovery processes, and more importantly, they provide findings that can be used to discuss the mechanisms that underlie VSN and its pathological structure.

DISCUSSION

It is evident that the wide range of symptomatic heterogeneity in patients with VSN is largely attributable to multi-component deficits including the widespread visuospatial attention network. We conducted the present study to establish the pathological structure of VSN by using a multivariate analysis and machine learning algorithms based on a variety of symptom-related evaluation parameters, and we sought to reveal the relationships between symptomatic features and the responsible brain areas. The results of the PCA revealed distinct four fundamental aspects of VSN: arousal and attention state, exogenous neglect, SWM, and attention bias. The GMM-based clustering detected six clusters that are reasonably characterized by the different contributions of the four PCs. These symptomatic characterizations were supported by the results of the subtraction analysis of overlapping lesions based on differences among the clusters that revealed specific neural correlates for each of these components. Moreover, the recovery process after unilateral spatial neglect (USN) was characterized by the transition from one cluster to another in accordance with the contribution of multiple components of VSN during each recovery period. Our results provide
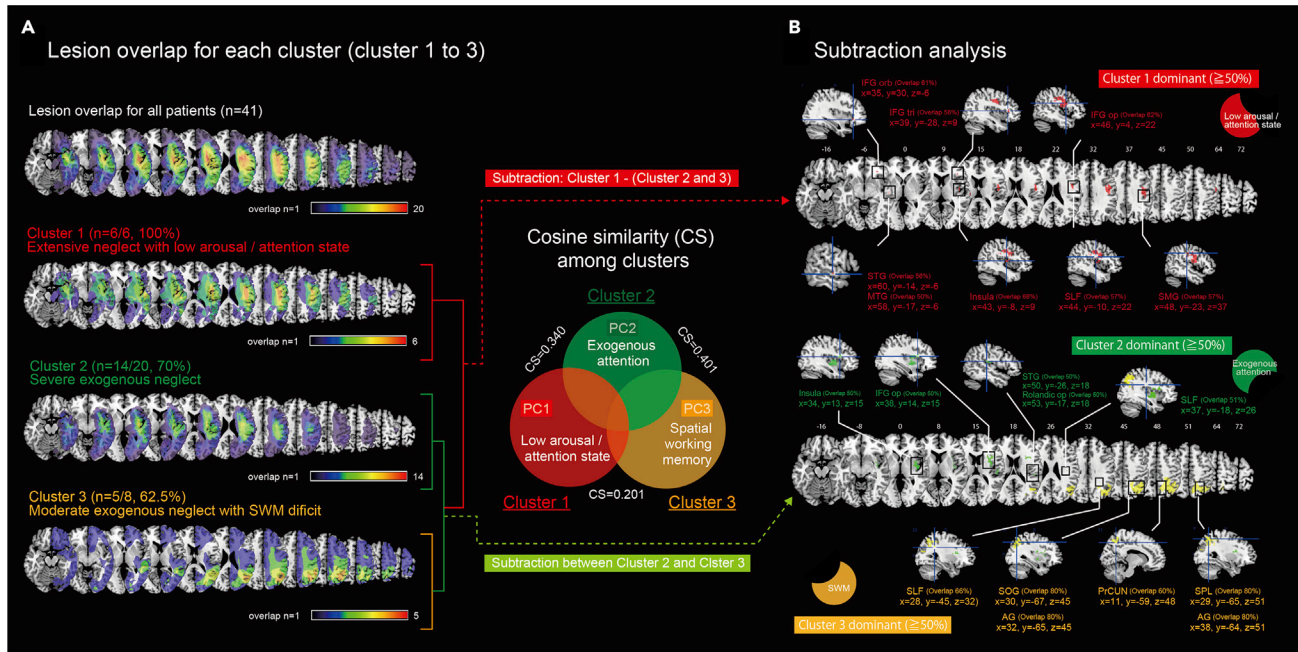
Figure 3. Lesion overlapping findings and the results of the subtraction analysis among clusters

(A) Top panel shows lesion overlapping among all 122 patients (n = 41). Bottom three panels show overlapping of clusters 1, 2, and 3. The Venn diagram is a schematic representation of the similarities/differences among three PCs based on the pairwise cosine similarity (CS) distances among clusters. The distance between the center of each circle reflects the CS value. The difference of each cluster clearly reflects distinct aspects of visuospatial neglect as follows: [arousal and attention state = cluster 1\(cluster 2 ∪ cluster 3), exogenous neglect = cluster 2\cluster 3, SWM = cluster 3\cluster 2]. We used this characterization for the subtraction analysis of the brain lesion overlapping, and we obtained the specific neural correlates for each of these components. (B) Top: The detected lesion by a subtraction of cluster 1 from clusters 2 plus 3. The dominant lesion areas (≧50%) are color highlighted in each brain map. Bottom: The detected lesion by subtraction between cluster 2 and cluster 3. The detailed results of the subtraction analysis are summarized in Table S3.

important point of view that the clinical manifestations of VSN might reflect a combination of distinct components affecting different aspects of spatial and non-spatial symptoms.

Four distinct components of visuospatial neglect and the relevant lesions

There is no single or perfect clinical evaluation for assessing VSN. It is speculated that there are distinct subtypes or different cognitive components underlying neglect symptom so that it is unlikely that damage to a unique area could explain clinical manifestations. To reveal the neural mechanisms underlying VSN, it is necessary to correctly understand the pathological structure based on various aspects of symptomatic characteristics behind spatial neglect. In the present study, we evaluated different aspects of elements of VSN, i.e., sustained attention, exogenous attention, endogenous attention, and SWM based on several parameters, and we attempted to break down neglect symptom into coherent profiles of co-varying deficits. We detected four principal components, and these four PCs can be interpreted as follows: PC1: arousal and attention state including sustained attention (Robertson et al., 1997; Rengachary et al., 2011; Robertson et al., 1998; Husain and Rorden, 2003) and exploratory neglect (Verdon et al., 2010) and severity of neglect. PC2: neglect with exogenous attention (Corbetta and Shulman., 2002; Corbetta and Shulman., 2011; Doricchi et al., 2008; Rengachary et al., 2011; Husain and Rorden., 2003; Posner et al., 1984). PC3: SWM deficit (Malhotra et al., 2009; Husain et al., 2001; Toba et al., 2018). PC4: attention bias (Bartolomeo et al., 2001; Azouvi et al., 2002).

In order to identify the lesions responsible for the above mentioned PCs, we attempted voxel-based lesion symptom mapping (VLSM: see Figure S2). The detected areas of arousal and attention state-related PC1 were the whole area of VAN (slightly frontal). Exogenous neglect-related PC2 had relevant lesions in the STG, middle temporal gyrus (MTG), and SLF. SWM deficit-related PC3 had relevant lesions in the dorsal occipitotemporal area. PC4 had a unique nature which showed both positive and negative variability reflecting left and right attention bias, respectively. The detected areas of the PC4 left attention bias-related
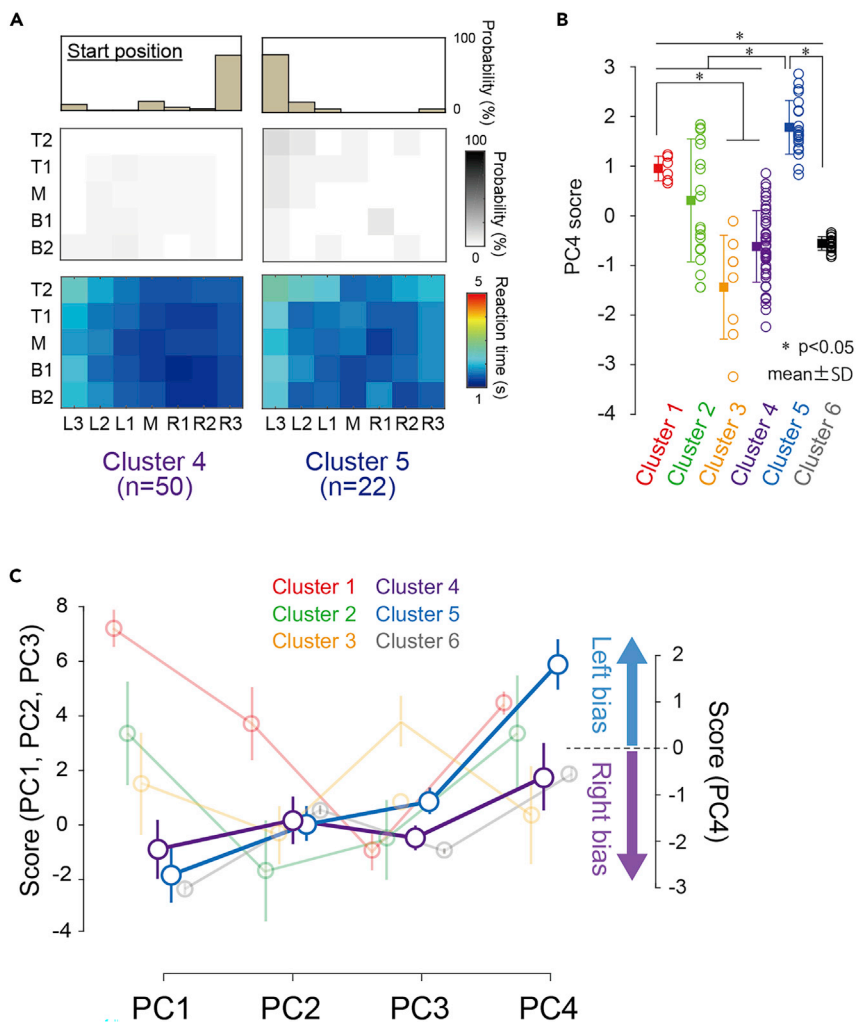
Figure 4. Component of attentional bias and selection strategy

(A) Results of EnAT and ExAT in cluster 4 and 5. While the probability of selection and reaction time were identical, initial selection (start position) shows clear difference between two clusters.

(B) Results of the statistical comparison of the scores among clusters, shown separately for each of the PC4. Data are represented as mean ± SD. Asterisks are represented as statistical significance (p < 0.05) to obtain by post hoc test (Steel-Dwass test) in Kruskal-Wallis test.

(C) Summarized in averaged PC score in each clusters. The difference between cluster 4 and 5 was particularly clear in PC4. Data are represented as mean ± SD.

positive score were the middle occipital gyrus (MOG), AG, and SOG. The PC4 right attention bias-related negative score had a relevant lesion in the STG. Although these results were based on uncorrected statistical level, the detected lesions are in good agreement with the previous reports. We then attempted a further process for the characterization of VSN with the GMM-based cluster analysis, and we then attempted to estimate neural correlates based on a subtraction analysis of the detected subtypes.

Six distinct subtypes of visuospatial neglect

With the PCA process, we were able to summarize the symptomatic nature of VSN as four principal components. Considering the wide heterogeneity, the nature of multiple components' deficits in VSN, we speculated that certain types of neglect consist of different contributions of each of the four components. We then attempted to detect the "subtypes" by conducting a GMM-based cluster analysis based on the PC score. GMM clustering is a probabilistic model-based clustering method and is more robust than other clustering methods (Banfield and Raftery 1993; Scrucca et al., 2016). The model with high theoretical validity
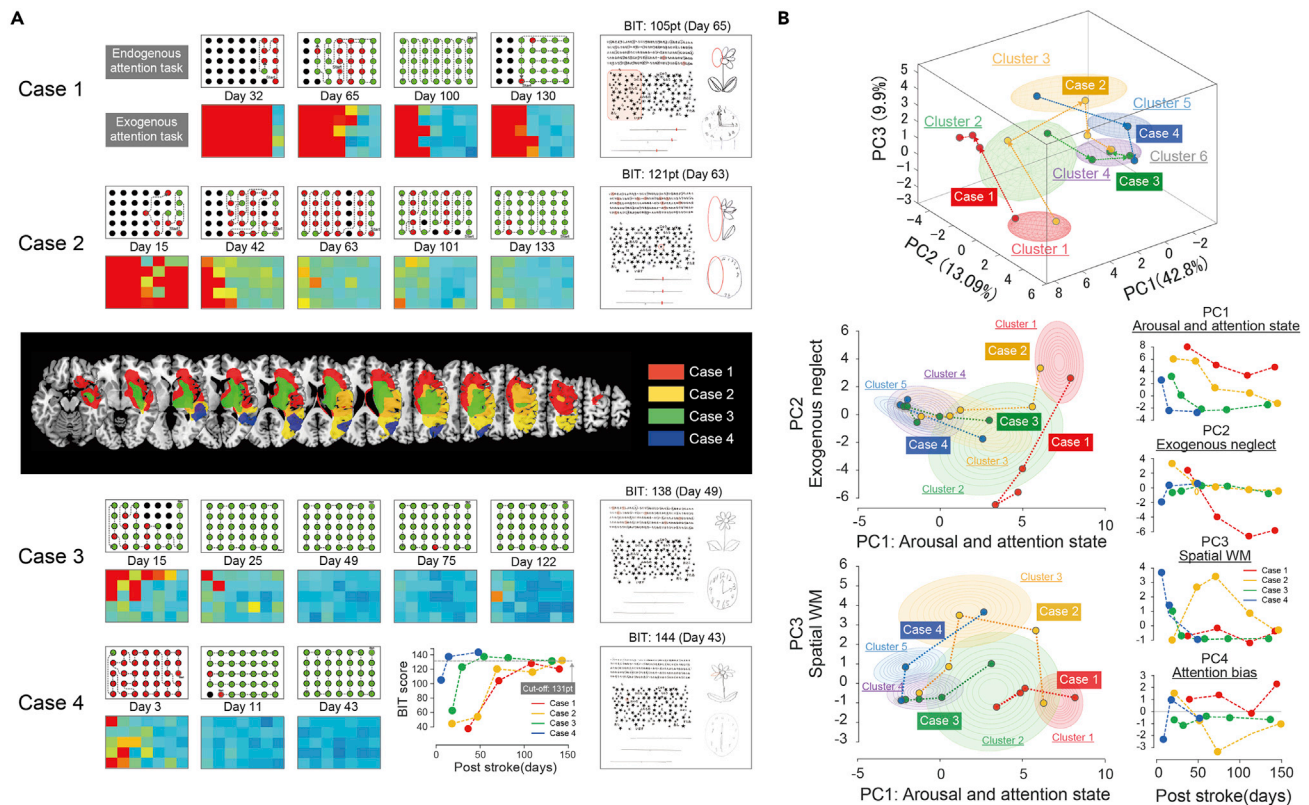
Figure 5. Longitudinal analysis in representative four patients

(A) In four representative cases, the results of a pair of EnAT and ExAT and BIT score were demonstrated. Middle MRI image is overlapping lesion of four cases. Time course changes in total score of BIT were summarized in the bottom of Figure 5A.

(B) Transition patterns among PCs in each case. This is a quantitative representation of the characteristic recovery process in representative cases (each case showed different traveling path). Contrast between case 1 and 2 seems to be clear that both cases originate from cluster 1 and then move to cluster 2 in case 1 (stagnation of exogenous attention) while move to cluster 3 in case 2 (SWM deficit). Contrast between case 3 and 4 reflects different aspect of recovery process, that is, both cases finally move to cluster 4, but originated from cluster 2 in case 3 (stagnation of exogenous attention) or from cluster 3 in case 4 (SWM deficit). These representative cases clearly demonstrated distinct modality of symptom and different recovery process and more importantly would give us materials to discuss mechanisms underlying visuospatial neglect and its pathological structure.

with better BIC and ICL values was selected as the optimal model from among several models that met these criteria. As summarized in Figure 2, we detected distinct six clusters. Each cluster was clearly explained by the relative contributions of the four PCs. Cluster 1 was characterized by extensive neglect with a low arousal/attention state as reflected by a high PC1 score. This cluster also reflected the severity of visuospatial attention. Cluster 2 was characterized by severe neglect with endogenous and exogenous attention, as reflected by a lower PC2 score. Cluster 3 had an at least partly common characteristic with cluster 2 (a moderate extent of exogenous neglect), but a distinct symptomatic nature could be identified, i.e., a deficit of SWM reflected by a high probability of re-selections. The component of attention bias (PC4) was clearly reflected by differences between clusters 4 and 5, which had similar contributions to PC1, 2, and 3 but exhibited rightward or leftward attention bias, respectively (Figure 4). Concerning this point, it was suggested that the initial selection position is a sensitive indicator in determining neglect symptoms (Azouvi et al., 2002). Our previous study also revealed that in patients who recognized their own neglect behavior, the patients tended to pay attention toward the left neglected space (Takamura et al., 2016). It is likely that the left bias reflects a compensatory strategy.

Neural correlates of visuospatial neglect

While the brain areas detected by VLSM were linearly correlated with a lesion with each component, those detected by the subtraction analysis can be regarded as specific lesions of each subtype. We observed the extent of common and different parts as quantified by cosine similarity. The Venn diagram in Figure 3 is a schematic representation of the differences among clusters 1, 2, and 3. We speculate that a portion of the

difference in each cluster might reflect distinct aspects of VSN as follows: [low arousal and attention state = cluster 1\(cluster 2 U cluster 3), exogenous neglect = cluster 2\cluster 3, SWM = cluster 3\cluster 2]. We used this characterization for the subtraction analysis of brain lesion overlapping, and then, we revealed specific neural correlates for each of these components.

Cluster 1 was interpreted as a cluster showing stagnation of endogenous/exogenous attention with an arousal decrease (a delayed response was also observed in the right space). Independent lesion locations were concentrated mainly in the insula and IFG, which is reported as an important site of convergence for stimulus-driven and goal-directed attention (Asplund et al., 2010). Concerning this point, Rencgachary et al. showed that patients with spatial neglect accompanying damage to the IFG showed severe neglect behavior and a delayed response of detection and re-orientation toward the right space (Rengachary et al., 2011). Moreover, the right insula has been associated with sustained attention (Thakral and Slotnick, 2009) and its damage causes a decrease in the improvement effect of attention to the neglected space from an auditory warning (Chica et al., 2012).

While clusters 2 and 3 showed a similar aspect of exogenous neglect, each had distinct symptomatic neglect behavior, namely, cluster 2 showed severe stagnation of exogenous attention, and cluster 3 showed SWM deficits (many re-cancellations in the overall space). The subtraction analysis of lesion over-laps between those two clusters revealed distinct lesion sites. Cluster 2 has lesions in the insula, IFGop, STG, and anterior parts of the SLF, which correspond to the disturbance of the VAN and contribute to the occurrence of USN and its chronicity (Thiebaut de Schotten et al., 2005; (Karnath et al., 2011); Lunven et al., 2015). In contrast, cluster 3 had lesions at the AG, SPL, SOG, precuneus, and posterior parts of the SLF. Damage to the medial parietal cortex was reported to cause disorder of spatial navigation such as global disorientation (Boccia et al., 2014; Aguirre and D'Esposito, 1999) and body awareness disorder (Her-bet et al., 2019; Wolpert et al., 1998). In addition, Cavanna and Trimble (Cavanna and Trimble., 2006) sug-gested that the precuneal cortex relates to self-related cognitive processes such as self-awareness, self-centered mental imagery strategies, social cognition, autobiographic memory, and others. Given these findings, it appears that the superior parietal area including the precuneal cortex is important for maintain-ing internal representations. Therefore, the symptom of cluster 3 can be characterized as an SWM deficit as a failure to maintain an internal representation for space between trans-saccadic updates. This interpreta-tion is in good agreement with reports that damage in the parietal cortex is related to SWM (Malhotra et al., 2009; Husain et al., 2001; Toba et al., 2018).

The schematic representation with Venn diagram in Figure 3 was inspired by Figure 2 in Husain's commen-tary (Husain, 2019). As one of the main components consists of VSN, Husain clearly placed selective atten-tion as direction bias in competition/in orienting attention. In our study, those components might have been involved in exogenous neglect and attention bias as revealed by PC2 and PC4, respectively. Through a comparison of results between VLSM and a subtraction analysis with the same patients, we identified an analysis procedure that can detect neural correlates behind VSN.

General discussion based on recovery process in four representative cases

As shown in the Figure 5, the longitudinal data clearly demonstrated that each patient exhibited improve-ment of the neglect symptom over time, but the symptomatic nature and the time course (i.e., the transition from one cluster to another) differed among the patients. Such time-dependent changes in the symptom-atic features were clearly characterized as transitions from one cluster to another, suggesting that some symptomatic characteristics could not be attributed to specific lesions.

Case 1, who showed clear stagnation of exogenous attention and remarkable left space neglect in BIT, could be regarded as having a higher probability of chronicity of VSN due to the disturbance of VAN (Thie-baut de Schotten et al., 2005; Karnath et al., 2011; Lunven et al., 2015). Case 2 had damage to the VAN and parietal cortex that may have caused neglect symptoms due to a failure of different components of spatial attention. The contrast between case 1 and 2 is a clear example of the distinct characteristics/subtypes of severe VSN. Interestingly, the difference in the contrast-recovery time course between cases 1 and 2 was clearly characterized as a form of transition among clusters. Case 3 and 4 are another pair showing different attention bias during their recovery. Both cases had a delayed reaction time on the ExoAT, but their behavior during the EndoAT was totally different: Case 3 lacked arousal and attention state as reflected by miss cancellations while case 4 showed extensive re-cancellation. Such different symptomatic natures

clearly reflect the process of recovery in each patient. While case 3 transited from cluster 2 to 4 as a type of rightward bias due to attention deficit, case 4 transited from cluster 3 to 5 as a type of compensatory leftward attention. Although they had a disturbance of VSN in the acute phase, both patients showed good recovery at 45 days after the onset of stroke and finally completed both the EndoAT and ExoAT without remarkable errors, and their BIT scores far exceeded the cutoff at 49 days in case 3 and 43 days in case 4. The contrast between case 3 and 4 is a clear example of distinct characteristics/subtypes of mild VSN.

As clearly shown in Figure 5B, manifestations of neglect symptom change with time. Moreover, as reflected in attention bias (PC4), the recovery process involves not only lesion-specific symptoms but also a compensatory strategy. Although several studies described the time course of the recovery from neglect symptom (Ramsey et al., 2016; Nijboer et al., 2013), no previous study had revealed the recovery process based on the characterization of VSN. The study is the first attempt to demonstrate the recovery process based on a comprehensive analysis of neglect symptom. Our results provide important information about the clinical manifestations of VSN that might reflect a combination of distinct components affecting different aspects of spatial and non-spatial symptoms. We therefore conclude that the process of a PCA and a PC score-based cluster analysis suitably classifies subtypes; in other words, the present results revealed the pathological structure of VSN.

Limitations and future direction

Further research is necessary to overcome the following limitations in the present study. First, we used only the overall score of the BIT. The results of paper-and-pencil tests essentially include the more detailed features of neglect symptom, e.g., the difference in the number of cancellations between the left and right in the cancellation task (Azouvi et al., 2002; Verdon et al., 2010), the characteristics of the copying task (Gainotti and Tiacci., 1970; Seki and Ishiai., 1996), a left hyperschemia (Rode et al., 2014), and others. Integrating these features may provide a more diverse and robust understanding of neglect symptoms. Second, in order to establish the pathological structure of VSN, we should attempt to establish a pathological model with structure estimated modeling with larger patient samples. Third, it is necessary to pay attention to the recovery process in order to establish a pathological model and responsible lesion for the symptomatic feature of VSN because a patient transits from one cluster to another during recovery as we showed in Figure 5. Most of the previous studies applied inclusion criteria of the identical recovery phase (i.e., acute phase or subacute and/or chronic phase), presumably because the neglect symptoms changed according to the neural reorganization and compensatory strategy during recovery. The present study strongly suggested that the symptomatic features gradually changed over the time course of recovery, even though the patient had an intrinsic/specific brain lesion. This might be one of the reasons why a PC score-based VLSM cannot detect specific lesions (we could only detect brain lesions by VLSM at the uncorrected statistical level). It is quite important that symptoms and neurological behavior not be directly correlated with specific brain areas. Elucidation of the qualitative differences in the changes of symptomatic features (i.e., PC scores and/or assigned clusters) during the recovery process by longitudinal studies is essential when detecting the lesions responsible for the symptomatic features of VSN. We regard this paper as a first step for a future progress, and we are planning to conduct prospective study and then establish rich data for both behavioral measures and brain image in order to overcome the above mentioned limitation of this study in the near future.

Resource availability

Lead contact

Information and requests for resources should be directed to and will be fulfilled by the lead contact. Noritaka Kawashima (nori@rehab.go.jp).

Materials availability

N/A.

Data and code availability

The data and code used in this study are available on request, in anonymized format, from the corresponding author.

METHODS

All methods can be found in the accompanying Transparent methods supplemental file.

REFERENCES

Aguirre, G.K., and D'Esposito, M. (1999). Topographical disorientation: a synthesis and taxonomy. Brain 122, 1613–1628.

Asplund, C.L., Todd, J.J., Snyder, A.P., and Marois, R. (2010). A central role for the lateral prefrontal cortex in goal-directed and stimulus-driven attention. Nat. Neurosci. 13, 507–512.

Azouvi, P., Samuel, C., Louis-Dreyfus, A., Bernati, T., Bartolomeo, P., Beis, J.M., Chokron, S., Leclercq, M., Marchal, F., Martin, Y., et al. (2002). Sensitivity of clinical and behavioural tests of spatial neglect after right hemisphere stroke. J. Neurol. Neurosurg. Psychiatr. 73, 160–166.

Banfield, J.D., and Raftery, A.E. (1993). Model-based Gaussian and non-Gaussian clustering. Biometrics 49, 803–821.

Bartolomeo, P., Siéroff, E., Decaix, C., and Chokron, S. (2001). Modulating the attentional bias in unilateral neglect: the effects of the strategic set. Exp. Brain Res. 137, 432–444.

Bartolomeo, P., Thiebaut de Schotten, M., and Chica, A.B. (2012). Brain networks of visuospatial attention and their disruption in visual neglect. Front. Hum. Neurosci. 6, 110.

Beauchamp, M.S., Petit, L., Ellmore, T.M., Ingeholm, J., and Haxby, J.V. (2001). A parametric fMRI study of overt and covert shifts of visuospatial attention. Neuroimage 14, 310–321.

Bisiach, E., Pizzamiglio, L., Nico, D., and Antonucci, G. (1996). Beyond unilateral neglect. Brain 119, 851–857.

Boccia, M., Nemmi, F., and Guariglia, C. (2014). Neuropsychology of environmental navigation in humans: review and meta-analysis of FMRI studies in healthy participants. Neuropsychol. Rev. 24, 236–251.

Cavanna, A.E., and Trimble, M.R. (2006). The precuneus: a review of its functional anatomy and behavioural correlates. Brain 129, 564–583.

Chica, A.B., Thiebaut de Schotten, M., Toba, M., Malhotra, P., Lupiáñez, J., and Bartolomeo, P. (2012). Attention networks and their interactions after right-hemisphere damage. Cortex 48, 654–663.

Corbetta, M., and Shulman, G.L. (2002). Control of goal-directed and stimulus-driven attention in the brain. Nat. Rev. Neurosci. 3, 201–215.

Corbetta, M., and Shulman, G.L. (2011). Spatial neglect and attention networks. Annu. Rev. Neurosci. 34, 569–599.

Corbetta, M., Ramsey, L., Callejas, A., Baldassarre, A., Hacker, C.D., Siegel, J.S., Astafiev, S.V., Rengachary, J., Zinn, K., Lang, C.E., et al. (2015). Common behavioral clusters and subcortical anatomy in stroke. Neuron 85, 927–941.

Doricchi, F., Thiebaut de Schotten, M., Tomaiuolo, F., and Bartolomeo, P. (2008). White matter (dis) connections and gray matter (dys) functions in visual neglect: gaining insights into the brain networks of spatial awareness. Cortex 44, 983–995.

Gainotti, G., and Tiacci, C. (1970). Patterns of drawing disability in right and left hemispheric patients. Neuropsychologia 8, 379–384.

Gitelman, D.R., Nobre, A.C., Parrish, T.B., LaBar, K.S., Kim, Y.H., Meyer, J.R., and Mesulam, M.M. (1999). A large-scale distributed network for covert spatial attention: further anatomical delineation based on stringent behavioural and cognitive controls. Brain 122, 1093–1106.

Guariglia, C., Padovani, A., Pantano, P., and Pizzamiglio, L. (1993). Unilateral neglect restricted to visual imagery. Nature 364, 235–237.

Herbet, G., Lemaitre, A.L., Moritz-Gasser, S., Cochereau, J., and Duffau, H. (2019). The antero-dorsal precuneal cortex supports specific aspects of bodily awareness. Brain 142, 2207–2214.

Hopfinger, J.B., Buonocore, M.H., and Mangun, G.R. (2000). The neural mechanisms of top-down attentional control. Nat. Neurosci. 3, 284–291.

Husain, M. (2019). Visual attention: what inattention reveals about the brain. Curr. Biol. 29, R262–R264.

Husain, M., and Rorden, C. (2003). Non-spatially lateralized mechanisms in hemispatial neglect. Nat. Rev. Neurosci. 4, 26–36.

Husain, M., Mannan, S., Hodgson, T., Wojciulik, E., Driver, J., and Kennard, C. (2001). Impaired spatial working memory across saccades contributes to abnormal search in parietal neglect. Brain 124, 941–952.

Karnath, H.O. (1988). Deficits of attention in acute and recovered visual hemi-neglect. Neuropsychologia 26, 27–43.

Karnath, H.O., Rennig, J., Johannsen, L., and Rorden, C. (2011). The anatomy underlying acute

versus chronic spatial neglect: a longitudinal study. Brain *134*, 903–912.

Karnath, H.O., and Rorden, C. (2012). The anatomy of spatial neglect. Neuropsychologia *50*, 1010–1017.

Kim, M.S., and Cave, K.R. (1999). Top-down and bottom-up attentional control: on the nature of interference from a salient distractor. Perception Psychophys. *61*, 1009–1023.

Lunven, M., Thiebaut de Schotten, M., Bourlon, C., Duret, C., Migliaccio, R., Rode, G., and Bartolomeo, P. (2015). White matter lesional predictors of chronic visual neglect: a longitudinal study. Brain *138*, 746–760.

Malhotra, P., Coulthard, E.J., and Husain, M. (2009). Role of right posterior parietal cortex in maintaining attention to spatial locations over time. Brain *132*, 645–660.

Nijboer, T.C., Kollen, B.J., and Kwakkel, G. (2013). Time course of visuospatial neglect early after stroke: a longitudinal cohort study. Cortex *49*, 2021–2027.

Posner, M.I., Walker, J.A., Friedrich, F.J., and Rafal, R.D. (1984). Effects of parietal injury on covert orienting of attention. J. Neurosci. *4*, 1863–1874.

Ramsey, L.E., Siegel, J.S., Baldassarre, A., Metcalf, N.V., Zinn, K., Shulman, G.L., and Corbetta, M. (2016). Normalization of network connectivity in hemispatial neglect recovery. Ann. Neurol. *80*, 127–141.

Rengachary, J., He, B.J., Shulman, G., and Corbetta, M. (2011). A behavioral analysis of spatial neglect and its recovery after stroke. Front. Hum. Neurosci. *5*, 29.

Robertson, I.H., Manly, T., Beschin, N., Daini, R., Haeske-Dewick, H., Hömberg, V., and Weber, E. (1997). Auditory sustained attention is a marker of unilateral spatial neglect. Neuropsychologia *35*, 1527–1532.

Robertson, I.H., Mattingley, J.B., Rorden, C., and Driver, J. (1998). Phasic alerting of neglect patients overcomes their spatial deficit in visual awareness. Nature *395*, 169–172.

Rode, G., Ronchi, R., Revol, P., Rossetti, Y., Jacquin-Courtois, S., Rossi, I., and Vallar, G. (2014). Hyperschematia after right brain damage: a meaningful entity? Front. Hum. Neurosci. *8*, 8.

Rosen, A.C., Rao, S.M., Caffarra, P., Scaglioni, A., Bobholz, J.A., Woodley, S.J., and Binder, J.R. (1999). Neural basis of endogenous and exogenous spatial orienting: a functional MRI study. J. Cognit. Neurosci. *11*, 135–152.

Saj, A., Verdon, V., Hauert, C.A., and Vuilleumier, P. (2018). Dissociable components of spatial neglect associated with frontal and parietal lesions. Neuropsychologia *115*, 60–69.

Scrucca, L., Fop, M., Murphy, T.B., and Raftery, A.E. (2016). Mclust 5: clustering, classification and density estimation using Gaussian finite mixture models. R. Journal *8*, 289.

Seki, K., and Ishiai, S. (1996). Diverse patterns of performance in copying and severity of unilateral spatial neglect. J. Neurol. *243*, 1–8.

Takamura, Y., Imanishi, M., Osaka, M., Ohmatsu, S., Tominaga, T., Yamanaka, K., Morioka, S., and Kawashima, N. (2016). Intentional gaze shift to neglected space: a compensatory strategy during recovery after unilateral spatial neglect. Brain *139*, 2970–2982.

Thakral, P.P., and Slotnick, S.D. (2009). The role of parietal cortex during sustained visual spatial attention. Brain Research *1302*, 157–166.

Thiebaut de Schotten, M., Urbanski, M., Duffau, H., Volle, E., Lévy, R., Dubois, B., and Bartolomeo, P. (2005). Direct evidence for a parietal-frontal pathway subserving spatial awareness in humans. Science *309*, 2226–2228.

Toba, M.N., Rabuffetti, M., Duret, C., Pradat-Diehl, P., Gainotti, G., and Bartolomeo, P. (2018). Component deficits of visual neglect:"Magnetic" attraction of attention vs. impaired spatial working memory. Neuropsychologia *109*, 52–62.

Verdon, V., Schwartz, S., Lovblad, K.O., Hauert, C.A., and Vuilleumier, P. (2010). Neuroanatomy of hemispatial neglect and its functional components: a study using voxel-based lesion-symptom mapping. Brain *133*, 880–894.

Wilson, B., Cockburn, J., and Halligan, P. (1987). Development of a behavioral test of visuospatial neglect. Arch. Phys. Med. Rehabil. *68*, 98–102.

Wolpert, D.M., Goodbody, S.J., and Husain, M. (1998). Maintaining internal representations: the role of the human superior parietal lobe. Nat. Neurosci. *1*, 529–533.

Supplemental information

Pathological structure of visuospatial

neglect: A comprehensive multivariate analysis

of spatial and non-spatial aspects

Yusaku Takamura, Shintaro Fujii, Satoko Ohmatsu, Shu Morioka, and Noritaka Kawashima

Supplemental Materials

TRANSPARENT METHODS

Participants

Five collaborative hospitals in Japan routinely administer a paper-and-pencil test and touch panel attentional tests (described below) for patients who have suffered a right hemisphere stroke. Both types of tests were taken by 305 patients who were treated at one of these five hospital during the period 2014–2017. For the present cross-sectional study, we retrospectively analyzed the data from the 122 patients who completed both tests and whose detailed data were available. The exclusion criteria were (1) a history of major psychiatric or neurological disorders and (2) the patient found it difficult to understand either test. The average time interval between stroke onset and the testing was 91.23 ± 190.09 days. The mean age of the patients was 66.37 ± 12.08 years. As the clinical routine for evaluating the extent of USN, the patients were scored by the BIT (Wilson et al., 1987) and the Catherine Bergego Scale (CBS; Bergego et al., 1995). In two neuropsychological tests, BIT was conducted for all patients, but CBS was conducted to 49 of 122 patients.

The study procedures and the potential risk of the personal computer (PC)-based evaluation were explained to each patient, and informed consent was obtained from all patients (or a relative of the patient if he or she could not completely understand the study's explanation) before study participation. This study was approved by the Ethics Committee of the National Rehabilitation Center for Persons with Disabilities, Saitama, Japan (reference no. 24-36) and conformed to the tenets of the Declaration of Helsinki.

Evaluation parameters

The patients performed a custom developed reaction time task (@Attention; Creact Corp., Tokyo) using a personal computer with a touch-panel display (21.5 inch), and they completed the Behavioural Inattention Test (BIT) for the evaluation of multiple components of neglect (Fig. 1). The objects of the task are 35 objects (12-mm-dia.) arranged in seven columns and five rows.

Endogenous attention task

The endogenous attention task (EndoAT, Fig. 1A, top) evaluated the patients' 'top-down' endogenous attention. The patient was asked to select all targets in any order (by touching the target on the display with an index finger). When the patient touched a target, the object flashed briefly and then recovered to the default black color. Before the initiation of a trial, the patient was instructed to touch all of the objects and finish when all targets were selected. The propriety of selection, with or without multiple selection (whether a single target was selected more than once), and the selection order (increasing in order from the top left of the display; if the patient could not select the target it was defined as 35 [top right]) were recorded for the later analysis. We quantified each of the six variables for the subsequent analysis (see Fig. 1A and Table 1). We performed the following three steps for the subsequent exploratory/data-driven analysis: a) dimensional reduction from 18 variables using PCA to elucidate the neglect-related deficit components; b) GMM-based probabilistic clustering using the four obtained PCs to elucidate different combinations of neglect-related components for each patient; and c) lesion overlap subtraction of each cluster and VLSM for the four obtained PCs in order to understand the neural mechanisms underlying the neglect-related symptomatic components.

Exogenous attention task

The exogenous attention task (ExoAT, Fig. 1A, middle) evaluated the patients' 'bottom-up' exogenous attention. Based on the randomized function of the software program (LabVIEW ver. 2012, National Instruments, Austin, TX, USA), one of the objects flashed on a 500-ms cycle (black/red alternative switching) until the patient chose it (touched it with an index finger). If the patient could not find the flashing object within 5 seconds, the flashing stopped, and the next object started flashing. Before the initiation of a trial, the patient was instructed to touch the flashing objects as quickly as possible and to not do anything if she/he did not see any flashing object. The propriety of selection and the reaction time required for the choice of each object were recorded in the PC for the later analysis.

Behavioral Inattention Test

The BIT is a conventional test (Fig. 1A, bottom) for evaluations of USN. It includes the following six tests: line cancellation test, letter cancellation test, star cancellation test, copying test, line bisection test, and drawing test. The points on each test were scored by a conventional evaluation method (Ishiai., 1999; Wilson et al.,1987).

Data analysis

Feature extraction based on behavioural test

To visually reveal the spatial distribution of the propriety of selection at both tasks (including reselection and selection order only in the EndoAT) and reaction time on the ExoAT in the 2D plane, we created a space-propriety and time diagram in three dimensions (x = line, y = row, z = propriety and reaction time). Based on the recorded and

scored parameters in both tasks, we quantified a total of 18 variables (Table 1).

The following 6 variables were calculated based on the results of EndoAT: 1) mis-selection count in overall space (MSc_Endo) relating to the general endogenous attention score; 2) the difference of mis-selection count between the left and right space (L-Rdiff_Endo) relating to the neglect in endogenous attention; 3) reselection rate in overall space (%ReSel) relating to the spatial working memory; 4) reselection rate in the left hemi space (%ReSel_L) relating to the spatial working memory in the left space; 5) the initial select position (InitialPos) relating to the attentional bias and exploratory strategy; and 6) the number of midline crossings (CrossMid) relating to the exploratory strategy.

 In the same way, we quantified the following 6 variables based on the results of ExoAT: 1) mis-selection count in the overall space (MSc_Exo) relating to the general exogenous attention score; 2) mean reaction time (RTmean), relating to sustained attention and arousal; 3) standard deviation of the reaction time (RTstd), relating to attentional variability and neglect; 4) difference of mis-selection count between the left and right space (L-Rdiff_Exo) relating to neglect in exogenous attention; 5) ratio of the reaction time in the left space to the reaction time in the right space (L/Rratio) relating to neglect in exogenous attention; 6) ratio of the reaction time for the left-end-column target to the reaction time for the right-end-column target (EndlineL/R) relating to neglect in exogenous attention.

In the BIT, the following 6 variables were scored by a conventional evaluation method (Ishiai., 1999; Wilson et al.,1987): 1) the score of the line cancellation test (BIT_Line); 2) the score of the letter cancellation test (BIT_Letter), 3) the score of the star cancellation test (BIT_Star); 4) the score of the line bisection test (BIT_Bisect); 5) the score of the copying test (BIT_Copy); 6) the score of the drawing test (BIT_Draw). In subsequent

analysis, six BIT scores were used with the sign reversed.

All feature extraction processes in EndoAT, ExoAT were performed using MATLAB software and custom scripts (ver. 2015a Mathworks, Natick, MA).

Gaussian mixture model clustering for principal components

The main goal of this study was to classify subtypes of USN consisting of multiple components from the differences in the pathological characteristics in neglect behavior. We thus performed a principal component analysis (PCA) as a common data reduction strategy for obtaining the elements of spatial and non-spatial attention. A PCA is designed to reduce the dimensionality of a data set consisting of many interrelated variables while retaining as much as possible of the variation present in the data set. This is achieved by transforming to a new set of variables, the principal components (PCs), which are uncorrelated, and which are ordered so that the first few PCs retain most of the variation present in all of the original variables. PCA was performed after standardization of all variables. The acceptance criteria of the PCs were defined using a parallel analysis, and the percent of cumulative proportion was >70%.

We then performed Gaussian mixture model (GMM)-based clustering using the acceptable PCs to classify the patients. GMM clustering is a probabilistic model-based clustering method and is more robust than other clustering methods (Banfield and Raftery., 1993). In this clustering approach, the number of clusters and differences in distribution and its volume, shape and orientation can also be compared with statistical information criteria such as the Bayesian information criterion (BIC) and/or integrated the complete-data likelihood (ICL) criterion (Scrucca et al., 2016). We defined the following two criteria for the number of clusters and distribution features: (1) the number of clusters is

3 to 7 (the aim was to provide a more detailed classification than the three categories of severe VSN, moderate USN and no USN), and (2) the model distribution parameter is not equal variance. The model with high theoretical validity with better BIC and ICL values was selected as the optimal model from among several models that met these criteria. GMM-based clustering has been reported to be useful for characterizing the recovery process on longitudinal evaluations in patients with gait disorders caused by stroke (Dolatabadi et al., 2016). That study applies the computation of cluster membership probabilities for each patient in this probabilistic clustering. In the present study, cases that could also be evaluated longitudinally were fit to the model for a clarification of the recovery process after USN. All clustering procedures were performed by the software program R 3.5.0. We also used the add-on packages of R called psych (Revelle., 2015) and mclust5 (Scrucca., 2016) for a parallel analysis to define the acceptable number of PCs and for the Gaussian mixture model clustering.

Statistical analysis

Differences in basic attributes and the neuropsychological test scores in each cluster were examined with the chi-squared test and Kruskal-Wallis test (post hoc Steel Dwass test). Statistical significance was accepted at $p < 0.05$. All statistical procedures were also performed by R 3.5.0.

Brain imaging and lesion analysis

Lesion analyses were performed based on the cranial scans (MRI and CT) in 41 of the 122 patients conducted at their final scan and used for diagnosis. The lesion analyses were performed by experienced brain imaging clinicians (YT, SF, SO). Images were converted

to NIfTI format, and stroke lesions were determined for each patient by drawing the lesion locations directly on the original T2, FLAIR and CT images using MRIcroN software, www.mccauslandcenter.sc.edu/mricro/mricron).

Individual cranial scans and the lesion locations were transferred into stereotaxic space using the normalization algorithm of SPM8 (http://www.fil.ion.ucl.ac.uk/spm) and the Clinical Toolbox (Rorden et al., 2012 (http://www.mricro.com/clinical-toolbox/spm8-scripts). Using the 'MR normalize' algorithm of the Clinical Toolbox, individual cranial scans and lesion locations were transformed to the T1 template based on older individuals with a resampled voxel size of 1 mm^3.

The lesion locations were then compared using the subtraction technique (Rorden and Karnath., 2004) for an investigation of the lesion differences between each cluster. This technique illustrates the nodal point of overlap among lesions associated with a disorder, in direct visual contrast to sites that are not associated with that disorder. The normalized lesion volumes of interest were overlaid on the T1-weighted template MRI-scan from the Montreal Neurological Institute (MNI, http://www.bi.mni.mcgill.ca).

To evaluate the lesion areas with respect to cortical and subcortical gray matter structures, we overlaid the maps on the Automated Anatomical Labelling atlas (Tzourio-Mazoyer et al 2002) distributed with MRIcron. To identify the white matter fiber tracts affected by the lesions, we overlaid the lesion maps with the white matter fiber tract templates from the Johns Hopkins University (JHU) white-matter tractography atlas (Wakana et al., 2007).

RESULTS

Relationships between the BIT and Touch panel-based test (Relevance to Figure 1)

Supplementary figure S1 shows the relationships between the behavioural inattention test and touch panel-based test. As shown in the below scatterplots (Supplementary figure S1B and S1C), the PC1-related variables, RTmean and MSc-Ex, showed strong correlation with BIT. These variables might reflect arousal and attention state. On the other hand, the PC2-related variables, L/Rratio and RTstd, showed weak correlation with BIT, suggesting that the BIT score did not include the exogenous aspect of visuospatial attention. The PC3-related variables, %ReSel, showed moderate correlation with BIT.

Optimal model selection in GMM-based clustering (Relevance to Figures 2 and 4)

Supplementary Table S1 provides the BIC and ICL values of the total of 60 models that met the criteria. For both the BIC and the ICL, Models 1, 2 and 3 were listed as the top three models. From the top three models in which the BIC and ICL are better, six classes with a VEE model (ellipsoidal distribution and variable volume, equal shape, equal orientation) were accepted as models with high theoretical validity.

Details of the lesion subtraction (Relevance to Figure 3)

Detailed results of the subtraction analysis of [Clusters 2–3] and [Cluster (1+2)-3] are listed in Supplementary Table S3. These results correspond to Figure 3 in the main manuscript.

Voxel-based lesion symptom mapping (Relevance to Figure 3)

Supplementary Fig. S2A illustrates the VLSM results regarding the three main

components detected by the PCA. The red-, green- and yellow-highlighted areas indicate statistically significant voxels with the respective PCs (uncorrected $p<0.05$) indicated in the figure. The detected areas of PC1 (arousal and attention state-related) were the insula $(x, y, z = 40, −12, 14)$, inferior frontal gyrus (IFG) (orb: 43, 10, 29, tri: 39, 30, 10), superior longitudinal fasciculus (SLF) (43, −14, 26), angular gyrus (AG) (45, −40, 30), superior temporal gyrus (STG) (46, −24, 15), and supramarginal gyrus (SMG) (50, −22, 26). The exogenous neglect-related PC2 had relevant lesions in the STG (45, −36, 13), middle temporal gyrus (MTG) (39, −48, 13) and SLF (40, −48, 13). The SWM deficit-related PC3 had relevant lesions in the AG (28, −57, 45), middle occipital gyrus (MOG) (31, −62, 39), superior occipital gyrus (SOG) (31, −67, 41), inferior parietal lobule (IPL) (32, −53, 48) and superior parietal lobule (SPL) (32, −55, 49). Supplementary Fig. S2B provides the VLSM results regarding PC4 separately, since this score showed both positive and negative variability, reflecting left or right attention bias. The areas detected for the PC4 left attention bias-related positive score were the MOG (33, −63, 35), AG (44, −70, 35) and SOG (26, −62, 33). The PC4 right attention bias-related negative score had a relevant lesion in the STG (54, −25, 10).

Detailed description of longitudinal cases (Relevance to Figure 5)

Case 1 showed clear stagnation of exogenous attention and remarkable left space neglect in BIT. Even at the fourth measurement (130 days after the onset of stroke), miss-cancellation on the left space remained in all tasks. Since the potential lesions were distributed across a wide range of VAN, we considered that Case 1 could be regarded as having a higher probability of chronicity of visuospatial neglect (Thiebaut de Schotten et al., 2005; Karnath et al., 2011; Lunven et al., 2015).

Case 2 also showed severe attention deficit at his first assessment but showed a gradual improvement in all tasks. However, SWM deficits (such as a higher percentage of re-cancellation in the EndoAT) were observed. Interestingly, the copying and drawing tasks showed an extensive lack of piece in the left space. The persistence of neglect after damage to the parietal cortex is often observed in a clinical context. Therefore, damage to the VAN and parietal cortex may cause neglect symptom due to a failure of different components of spatial attention. The contrast between Case 1 and 2 is a clear example of distinct characteristics/subtypes of severe visuospatial neglect.

Case 3 had a delayed reaction time on the ExoAT, which was presumably due to a lack of arousal and attention state, as reflected by the miss-cancellations. Although Case 3 had a disturbance of visuospatial neglect in the acute phase, this patient showed good recovery at 45 days after the onset of stroke and finally completed both the EndoAT and ExoAT without remarkable errors, and the BIT scores of this patient far exceeded the cut-off at 49 days. Case 3 transited from Cluster 2 to Cluster 4 as a type of rightward bias due to attention deficit.

Case 4 had a delayed reaction time on the ExoAT and showed extensive re-cancellation on the EndoAT. Similar to Case 3, this patient showed good recovery after the onset of stroke and finally completed both the EndoAT and ExoAT without remarkable errors, and the BIT scores of this patient far exceeded the cut-off at 43 days. In contrast to Case 3, Case 4 transited from Cluster 3 to Cluster 5 as a type of compensatory leftward attention. The contrast between Cases 3 and 4 provides a clear example of the distinct characteristics/subtypes of mild visuospatial neglect.

Supplementary Table S1. BIC and ICL in each model, Related to Figure 2 and Figure 4

Bayesian Information Criterion (BIC):

Number of clusters	EEI	VEI	EVI	VVI	EEE	EVE	VEE	VVE	EEV	VEV	EVV	VVV
3 Clusters	1848.16	1613.88	1781.98	1620.40	1783.23	1734.43	1630.03	1588.29	1678.47	1545.14	1676.50	1562.66
4 Clusters	1737.05	1555.66	1755.32	1586.66	1807.01	1772.51	1569.96	1538.77	1721.55	1502.08	1717.77	1513.03
5 Clusters	1693.80	1560.82	1712.09	1598.58	1846.99	1576.44	1575.78	1542.81	1725.14	1532.84	1748.59	1545.85
6 Clusters	1715.64	1530.38	1740.18	1580.18	1627.22	1619.70	1519.95	1528.03	1679.71	1529.61	1712.42	1558.06
7 Clusters	1674.34	1540.32	1719.84	1584.46	1589.86	1671.73	1526.19	1541.99	1726.35	1532.19	1746.78	1599.65

Integrated Complete-data Likelihood (ICL) criterion:

Number of clusters	EEI	VEI	EVI	VVI	EEE	EVE	VEE	VVE	EEV	VEV	EVV	VVV
3 Clusters	1858.57	1622.27	1788.14	1632.94	1788.23	1789.26	1636.51	1592.72	1683.96	1552.85	1688.71	1569.41
4 Clusters	1741.34	1564.91	1798.87	1596.88	1870.36	1887.74	1577.61	1546.32	1777.70	1509.07	1730.05	1521.75
5 Clusters	1702.93	1574.30	1719.38	1608.11	1906.00	1617.32	1588.50	1551.10	1781.92	1538.90	1828.79	1553.87
6 Clusters	1778.93	1537.95	1794.43	1589.62	1635.70	1680.54	1530.25	1534.05	1689.30	1536.12	1786.88	1565.17
7 Clusters	1683.10	1556.44	1728.61	1599.57	1596.31	1753.34	1536.74	1553.16	1756.95	1541.80	1788.13	1612.15

Underlining indicates the top three models.

Abbreviation: EEI: diagonal, equal volume and shape model, VEI: diagonal, varying volume, equal shape, EVI: diagonal, equal volume, varying shape, VVI: diagonal, varying volume and shape, EEE: ellipsoidal, equal volume, shape, and orientation, EVE: ellipsoidal, equal volume and orientation , VEE: ellipsoidal, equal shape and orientation, VVE: ellipsoidal, equal orientation, EEV: ellipsoidal, equal volume and equal shape, VEV: ellipsoidal, equal shape, EVV: ellipsoidal, equal volume, VVV: ellipsoidal, varying volume, shape, and orientation

Supplementary Table S2. Multiple comparisons, Related to Figure 2 and Figure 4

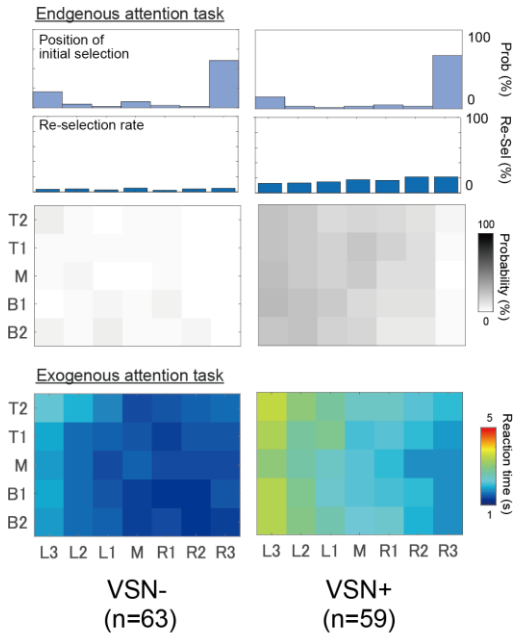| Steel-Dwass		PC1		PC2		PC3		PC4	
Cluster		p-value	r	p-value	r	p-value	r	p-value	r
Cls1 vs.	Cls2	0.015872	0.473	0.005553	0.544	0.999996	0.000	0.883335	0.029
Cls1 vs.	Cls3	0.023877	0.604	0.023877	0.604	0.023877	0.604	0.023877	0.604
Cls1 vs.	Cls4	0.000999	0.440	0.000999	0.440	0.605568	0.069	0.001381	0.427
Cls1 vs.	Cls5	0.003009	0.561	0.003009	0.561	0.003009	0.561	0.012278	0.473
Cls1 vs.	Cls6	0.00539	0.593	0.00539	0.593	0.930924	0.018	0.00539	0.593
Cls2 vs.	Cls3	0.351685	0.176	0.294882	0.198	0.000832	0.632	0.050205	0.370
Cls2 vs.	Cls4	3.96E-09	0.703	0.000273	0.435	0.581807	0.066	0.064736	0.221
Cls2 vs.	Cls5	4.5E-07	0.779	0.005643	0.427	0.005643	0.427	0.00515	0.432
Cls2 vs.	Cls6	5.21E-06	0.759	0.000854	0.556	0.990721	0.002	0.303393	0.172
Cls3 vs.	Cls4	0.007403	0.352	0.793254	0.034	9.48E-05	0.513	0.276959	0.143
Cls3 vs.	Cls5	0.002017	0.564	0.959201	0.009	0.000525	0.633	0.000525	0.633
Cls3 vs.	Cls6	0.001248	0.659	0.064817	0.377	0.001248	0.659	0.104183	0.332
Cls4 vs.	Cls5	0.014007	0.290	0.913258	0.013	3.09E-09	0.698	2.89E-10	0.743
Cls4 vs.	Cls6	4.99E-06	0.562	0.498077	0.083	6.39E-05	0.492	0.991165	0.001
Cls5 vs.	Cls6	0.831127	0.035	0.011953	0.408	2.91E-06	0.759	2.91E-06	0.759

Abbreviation: Cls: Cluster, PC: Principal component

Supplementary Table S3. Details of subtraction analysis, Related to Figure 3

Cluster 1 dominant areas (vs. Cluster 2 and Cluster 3)		
Area	**%Overlap**	**Atlas**
Precentral	73%	AAL
Postcentral	68%	AAL
Insula	68%	AAL
Rolandic_Oper	68%	AAL
Frontal_Inf_Oper	62%	AAL
Frontal_Inf_Orb	61%	AAL
SupraMarginal	57%	AAL
Superior_longitudinal_fasciculus	57%	JHU
Frontal_Inf_Tri	56%	AAL
Temporal_Sup	56%	AAL
Heschl	52%	AAL
Frontal_Mid	51%	AAL
Temporal_Mid	51%	AAL
Cluster 2 dominant areas		
Area	**%Overlap**	**Atlas**
Putamen	71%	AAL
External_capsule	64%	JHU
Insula	64%	AAL
Temporal_Sup	57%	AAL
Superior_longitudinal_fasciculus	51%	JHU
Superior_corona_radiata	51%	JHU
SupraMarginal	50%	AAL
Posterior_corona_radiata	50%	JHU
Frontal_Inf_Oper_R	50%	AAL
Anterior_corona_radiata	50%	JHU
Rolandic_Oper_R	50%	AAL
Heschl_R	50%	AAL
Cluster 3 dominant areas		
Area	**%Overlap**	**Atlas**
Angular	80%	AAL
Parietal_Sup	80%	AAL
Occipital_Sup	80%	AAL
Temporal_Mid	73%	AAL
Occipital_Mid	73%	AAL
Parietal_Inf	73%	AAL
Superior_longitudinal_fasciculus	66%	JHU
SupraMarginal	66%	AAL
Precuneus	60%	AAL
Temporal_Sup	59%	AAL
Posterior_corona_radiata	53%	JHU
Postcentral	53%	AAL
Cuneus	53%	AAL
Paracentral_Lobule	53%	AAL

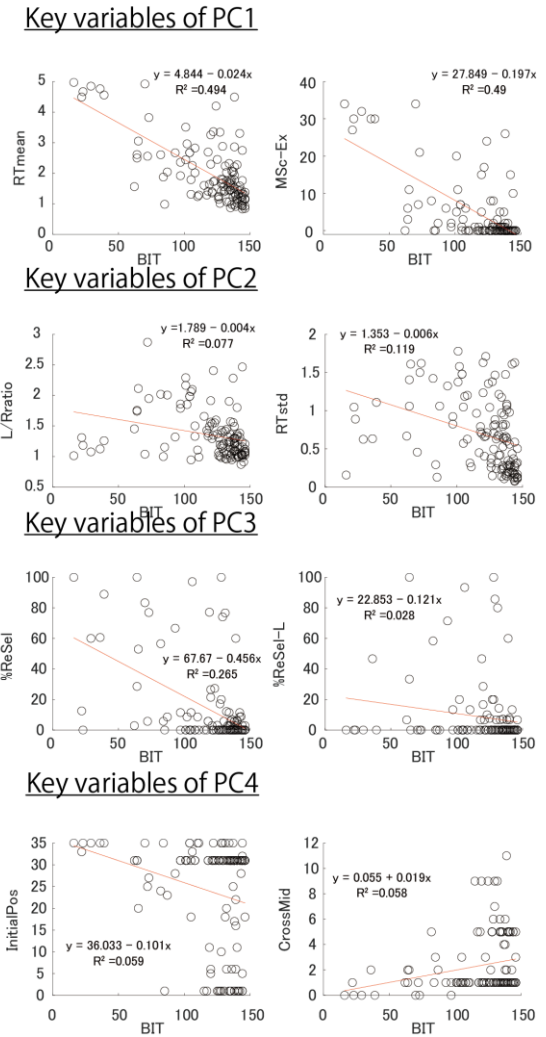Abbreviation: AAL: Automatic anatomical labeling, JHU: Johns Hopkins University white-matter tractography atlas

**A Summary of EndoAT and ExoAT in VSN+ and VSN- group**

Endegenous attention task

Position of initial selection

Re-selection rate

Exogenous attention task

VSN-
(n=63)

VSN+
(n=59)

B Relationships between BIT and key variables of PCs

Key variables of PC1

$y = 4.844 - 0.024x$
$R^2 = 0.494$

$y = 27.849 - 0.197x$
$R^2 = 0.49$

Key variables of PC2

$y = 1.789 - 0.004x$
$R^2 = 0.077$

$y = 1.353 - 0.006x$
$R^2 = 0.119$

Key variables of PC3

$y = 67.67 - 0.456x$
$R^2 = 0.265$

$y = 22.853 - 0.121x$
$R^2 = 0.028$

Key variables of PC4

$y = 36.033 - 0.101x$
$R^2 = 0.059$

$y = 0.055 + 0.019x$
$R^2 = 0.058$

C Correlation analysis

	VarName	r	p
PC1	RTmean	-0.703	1.85E-19
	MSc_Ex	-0.700	2.89E-19
PC2	L/Rratio	-0.277	0.0020031
	RTstd	-0.345	9.89E-05
PC3	%ReSel	-0.514	1.35E-09
	%ReSel_L	-0.168	0.0651279
PC4	InitialPos	-0.242	0.0071518
	CrossMid	0.241	0.0074554

Supplementary Figure S1, Related to Figure 1. A: Summary of EndoAT and ExoAT in patients with VSN+ and VSN+. Presence of VSN was defined using the cut-off score of the behavioural inattention test (BIT). All plots are constructed in a manner similar to that described in Figure 2D. The top row shows the position of the initial selection in EndoAT. The second row shows the reselection rate in EndAT. The third row shows the spatial distribution of the selection probability for each target in EndAT. The bottom row shows the spatial distribution of reaction time in ExoAT. **B**: Scatterplot showing the relationship between BIT and the key variables of four PCs. **C**: Correlation analysis between BIT and the key variables of four PCs.
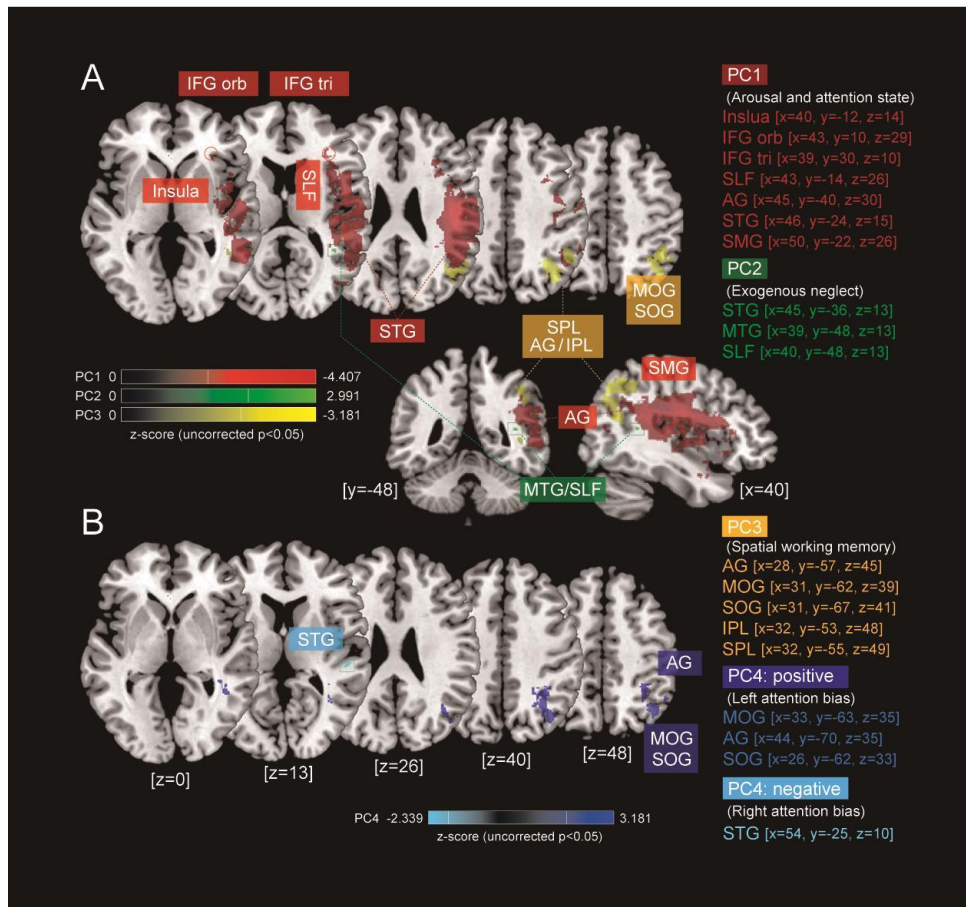
Supplementary Figure S2, Related to Figure 3. The VLSM results regarding the main components detected by the PCA. **A:** Red-, green- and yellow-highlighted areas indicate the voxels significantly correlated with PC1, PC2, and PC3, respectively (uncorrected p<0.05). **B:** VLSM results were determined separately for PC4, because the score for this component showed both positive and negative variability, reflecting the left and right attention bias, respectively. The areas highlighted in dark blue and light blue indicate voxels significantly correlated with positive and negative PC4 scores, respectively (uncorrected p<0.05).

Supplemental References

Bergego, C., Azouvi, P., Samuel, C., Marchal, F., Louis-Dreyfus, A., Jokic, C., Morin, L., Renard, C., Pradat-Diehl, P., Deloche, G. (1995). Validation d'une échelle d'évaluation fonctionnelle de l'héminégligence dans la vie quotidienne: l'échelle CB. Ann. Readapt. Med. Phys. 38, 183-9.

Dolatabadi, E., Mansfield, A., Patterson, K. K., Taati, B., and Mihailidis, A. (2016). Mixture-model clustering of pathological gait patterns. IEEE J. Biomed. Health. Inf. 21, 1297-1305.

Ishiai, S. (1999). Behavioural Inattention Test. Japanese Version. Sinko Igaku Syuppan, Japan.

Revelle, W., and Revelle, M. W. (2015). Package 'psych'. The comprehensive r archive network.

Rorden, C., Bonilha, L., Fridriksson, J., Bender, B., and Karnath, H. O. (2012). Age-specific CT and MRI templates for spatial normalization. Neuroimage 61, 957-965.

Rorden, C., and Karnath, H. O. (2004). Using human brain lesions to infer function: a relic from a past era in the fMRI age?. Nat. Rev. Neurosci. 5, 812-819.

Scrucca, L., Fop, M., Murphy, T. B., and Raftery, A. E. (2016). mclust 5: clustering, classification and density estimation using Gaussian finite mixture models. The R journal 8, 289.

Tzourio-Mazoyer, N., Landeau, B., Papathanassiou, D., Crivello, F., Etard, O., Delcroix, N., ... and Joliot, M. (2002). Automated anatomical labeling of activations in SPM using a macroscopic anatomical parcellation of the MNI MRI single-subject brain. Neuroimage 15, 273-289.

Wakana, S., Caprihan, A., Panzenboeck, M. M., Fallon, J. H., Perry, M., Gollub, R. L., ...

and Mori, S. (2007). Reproducibility of quantitative tractography methods applied to cerebral white matter. Neuroimage 36, 630-644.

Wilson, B., Cockburn, J., and Halligan, P. (1987). Development of a behavioral test of visuospatial neglect. Arch. Phys. Med. Rehabil. 68, 98-102.